

Advances In Two-Fluid Model CFD Simulation For Fluidized Bed Gasifier

Raj kumar^{1*}, Narayan Lal Panwar¹, Vinod Kumar², Manjeet Singh³, Sanwal Singh Meena⁴, Kalpana Jain⁵

¹Department of Renewable Energy Engineering, MPUAT, Udaipur (Rajasthan), 313001, India

²Department of Electrical Engineering, MPUAT, Udaipur (Rajasthan), 313001, India

³Department of Soil and Water Engineering, MPUAT, Udaipur (Rajasthan) 313001, India

⁴Department of Farm machinery and power Engineering, MPUAT, Udaipur (Rajasthan) 313001, India

⁵Department of Computer science Engineering, MPUAT, Udaipur (Rajasthan), 313001, India

*Corresponding author: rajkumardorwal@gmail.com

Abstract:

For sustainable development to overcome the world environmental problems, use of biomass for renewable energy generation is one of the most prominent solutions. The gasification process for biomass degradation using gasifiers is one of the most promising techniques. For designing an efficient system there is a need of comprehensive analysis of heat and mass transfer processes in gasifier. Computational Fluid Dynamics (CFD) simulations are an invaluable tool to analyze the efficiency, accuracy and micro level optimization of all processes involved in gasification. This review delves into the advancements in Computational Fluid Dynamics (CFD) simulations utilizing a two-fluid model for fluidized bed gasifiers. The paper highlights the importance of accurately representing gas compositions, species concentrations, and devolatilization processes within the reactor. The study has focused on use of CFD model to incorporate tar generation, comprehensive devolatilization procedures, and various reaction mechanisms for heterogeneous and homogeneous reactions. The study involves the comparison of different biomass types under varying operational parameters revealed insights into gasification processes. The review highlights the predictive capabilities of the two-fluid model by integrating advanced sub-models for interfacial momentum, particle interactions, and heat/mass transport. The integration of multi-scale simulation methods offers a comprehensive approach to capturing key aspects of gas-solid flow dynamics. Overall, this review paper contributes to the optimization of fluidized bed reactor design and the understanding of complex gas-solid interactions in industrial applications.

1. INTRODUCTION:

Environmental degradation and the energy crisis stand as paramount concerns in the pursuit of sustainable development [1]. Over the latter half of the 20th century, global efforts have coalesced to mitigate greenhouse gas emissions. These endeavors have materialized in organized international initiatives with the overarching aim of constraining the rise in the world's average temperature to within 3 °C above preindustrial levels [2]–[4]. The size of the worldwide biomass power generating industry is projected to increase by 39.21 GW between 2020 and 2024. This growth is driven by the increasing demand for renewable energy sources and the recognition of biomass as a sustainable and carbon-neutral fuel option. The adoption of biomass power as a renewable energy source is accelerating, leading to significant projected expansion in the global biomass power generating industry between 2020 and 2024 [5]. Fluidized beds find widespread use in chemical and process industries as a type of multiphase arrangement. Normally, they are made up of an upright container that holds solid particles. A porous plate or nozzles allow gas to enter from the bottom. This interaction between the gas and solid particles leads to fluidization, causing the bed to transition from a static to a fluid-like state and enhancing contact between the gas and solids. Several factors such as properties of the solid particles (shape, size, characteristics), bed geometry, distributor type, and gas properties (temperature, pressure, velocity) influence the process of fluidization. It is crucial to thoroughly comprehend this system in order to effectively design reactors and manage heat and mass transfer processes.

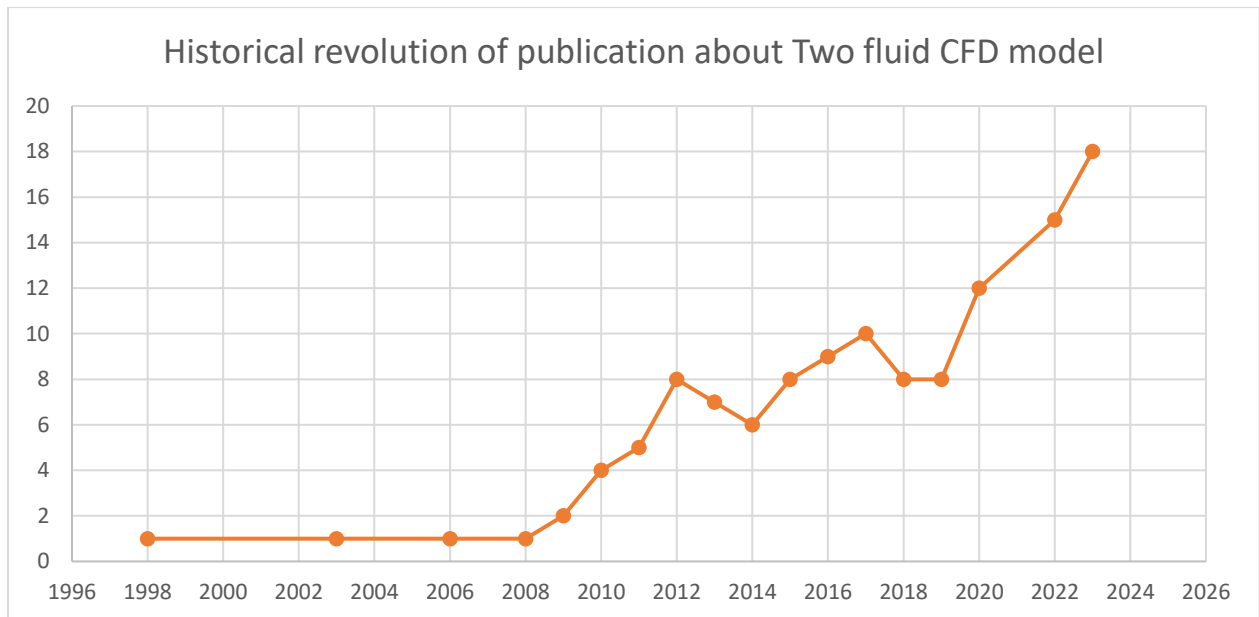


Fig 1: Historical evolution of SCOUPS publication about Two fluid CFD model

The two-stage technique relies on solving the volume-averaged Navier-Stokes equations for both the gas and solid components, incorporating relevant closure relationships to address their interaction. The gaseous state is characterized by the continuity and momentum equations, whereas the solid phase is defined by its distinct characteristics of these equations. The interaction between these two phases involves exchange terms for interphase momentum, taking into account drag force, lift force, and other forces acting between the phases.

The two-fluid model encompasses the following essential elements:

- The solid phase is considered as a unified entity with its unique speed, mass, and other characteristics.
- Accounting for the exchange of mass and momentum among the phases of gas and solidity is done through interphase exchange coefficients.
- Closure models are essential for determining parameters like solid pressure, solid shear stress, and gas-solid drag.
- The model has the potential for further improvement through the incorporation of additional physical phenomena, such as heat transfer, chemical reactions, and particle size distribution.
- Computational fluid dynamics (CFD) techniques may be employed to solve the model and predict hydrodynamics, heat and mass transport, and reaction kinetics inside the system of fluidized bed.
- The accuracy of the two-phase model relies on correctly choosing the closure models and implementing them numerically.

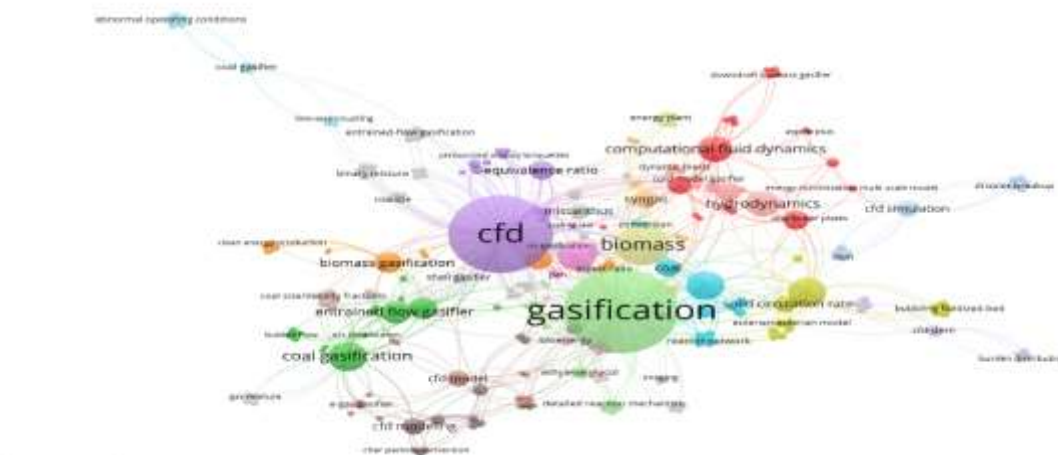


Fig 2: Co-word analysis, prepared using VOS viewer

In the study of fluidization, understanding the categorization of particles is crucial for predicting their behavior. Geldart [6] Based on their fluidization behavior at room temperature, particles are classified into four groups: B (sand-like or bubbling), D (coarse or spoutable), A (aeratable), and C (cohesive). A widely used empirical map employs Sauter diameter (mean) of particles in μm and gas-solid phase densities in kg/m^3 to examine gas-solid flow patterns (Fig. 1.1(b)) [7]. The transition from one particle classification to another can be explained using suitable equations that take into account these factors. Different fluidization patterns, including stationary beds, bubbling fluidized beds, and circulating fluidized beds, are visually distinguishable. These distinctions are illustrated in Fig. 1(a). Zhang and colleagues have formulated practical equations for calculating the velocity of fluidization at the boundaries between successive patterns [8]. To comprehend the heat transfer and mass transfer processes taking place within the reactor, it is essential to have a thorough grasp of the fluidization regime. A comprehensive map of flow regime that characterizes gas-particle mixer has been formulated and expanded upon by Reh [9], Grace [10], and Kunii & Levenspiel [11]. This map serves as a tool for identifying the fluidization regime (see Figure 1(c)). The graphic displays the Archimedes number on the x-axis and the particle Reynolds number on the y-axis. The classification of Geldart particles is denoted by A, B, C, and D. The application of the dual-fluid model has been instrumental in advancing the understanding and prediction of complex multiphase flows in various industrial applications. Over time, researchers have developed experimental methods to determine important parameters in small-scale tests on fluidized-bed reactors. These parameters include the minimum velocity for fluidization, formation of bubbles, erosion of particles, and distribution of solid mass along the reactor's axis [11]. While numerical simulation is a rapid and effective way to analyze local and global flow variables at an industrial level, its reliability for The development of extensive fluidized bed setups is restricted by a lack of understanding regarding essential gas-solid flow mechanisms, including interactions between gas and particles, among particles, and with the reactor walls. This challenge stems from significant differences in scales; macroscopic flow structures occur at the size of reactors while fundamental gas-solid flows take place at microscopic levels [12]. Ongoing research in this field aims to further improve the predictive capabilities of the two-fluid model by incorporating more advanced sub-models for interfacial momentum, details of particle-particle and particle-wall interaction, as well as heat and mass transport. In order to address the significant differences in scales within fluidized-bed systems, a multi-scale simulation method has been developed by researchers. This approach integrates four levels of physical mechanisms at different resolutions [13]–[15]. The method involves using smaller-scale models to establish closure relations that can be applied to larger-scale models. While experiments have demonstrated that these relations effectively capture the key aspects of gas-solid flow, there may be limitations in fully capturing all the underlying mechanisms of gas-solid interactions across various scales [12]. Figure 1.2 presents a diagram showing the four simulation models utilized in this comprehensive approach: quasi-single-phase techniques, discrete-particle techniques, two-fluid models, and direct numerical simulation.

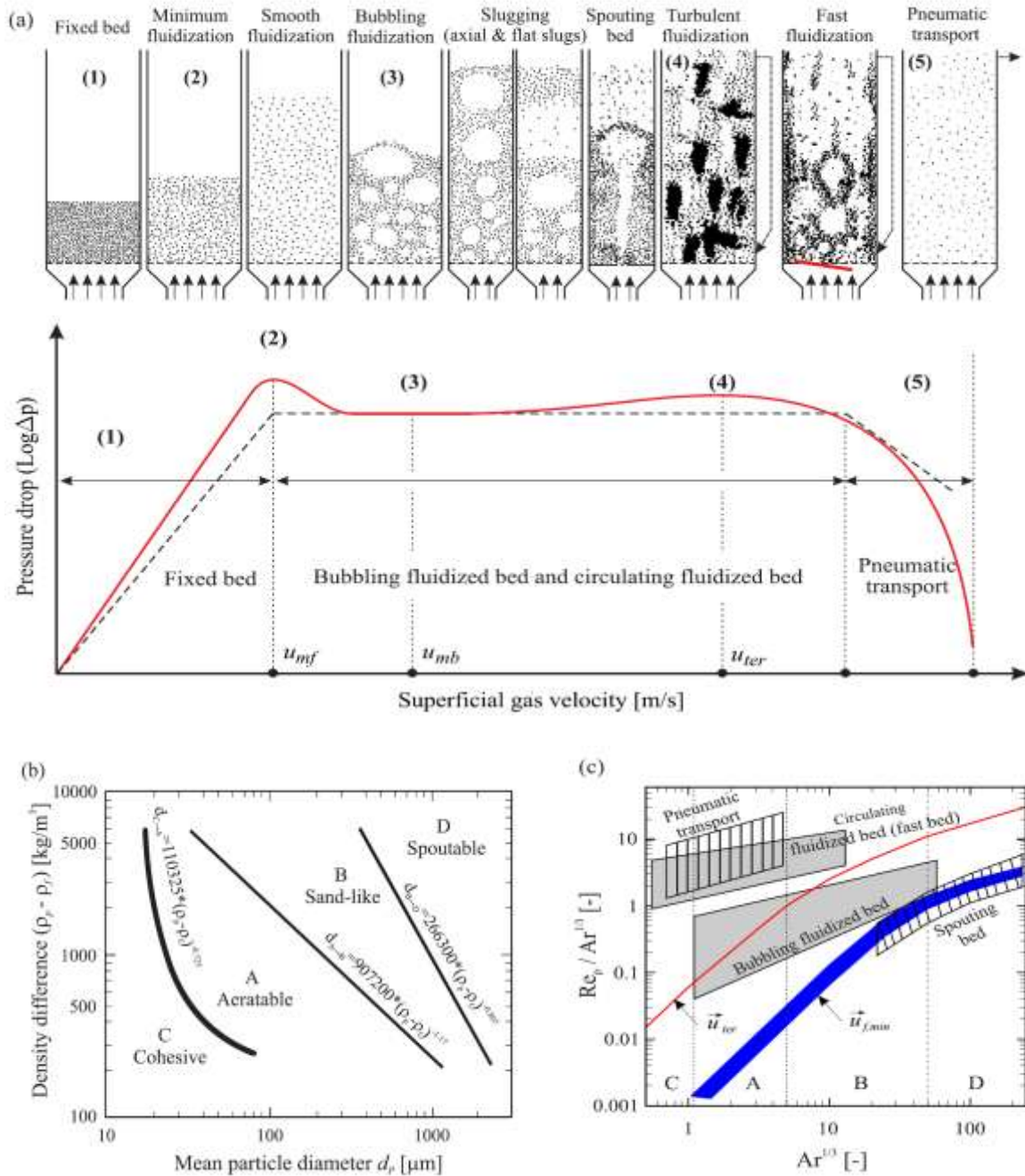


Fig. 3. a) Presser drop vs superficial velocity and fluidized regimes; dotted line represents an ideal bed, solid line represents the actual bed [11] b) particle categorization as described by Geldart [6] c) Fluidized bed regime map created by Reh & Grace [9]-[11]

2. Numerical model:

Numerical simulations have become increasingly crucial in the analysis and development of gas-solid flows, as well as in supplementing experimental data, due to advancements in computational capabilities. Various techniques have been developed to precisely depict the interactions. The interactions between gas and solid phases, as well as between particles and walls, involve various coupling methods. These consist of the following: the gas \rightarrow particle one-way dispersion phase model; the gas \leftrightarrow particle two-way coupling; the gas \leftrightarrow particle/wall \leftrightarrow particle four-way coupling; and a suggested three-way coupling technique (gas \leftrightarrow particle \leftrightarrow particle) by Loth et al. [16]. The selection of which technique to employ is contingent on The solid phase's volume fraction. The one-way coupled method is appropriate for the dilute gas-solid

flows. with a low solid volume fraction ($\epsilon_p < 10^{-6}$), where particle influence on flow turbulence is insignificant. For higher solid volume fractions ($10^{-6} \leq \epsilon_p < 10^{-3}$), it's recommended to use the two-way coupled approach since momentum exchange begins to affect gas flow structure. As for even higher solid volume fractions ($\epsilon_p > 10^{-3}$), employing a four-way coupled approach becomes necessary as various interactions start playing a significant role. The discrete-particle model, the hybrid model, the two-fluid model, and the direct numerical simulation model are some of the computational fluid dynamics methods that may be used to simulate gas-solid fluxes [17], [18].

3. Mathematical modeling:

Chemical and energy systems encompass intricate processes that encompass various phenomena, like thermo-chemical reactions and multi-phase flows. These flows consist of a minimum of two distinct phases with diverse material properties, the phase boundary distinctly separates these two regions. Different materials result in varied types of dual-phase flows -meet three kinds of flows: gas-fluid, fluid-solid, and gas-solid, in the fluidized bed systems, in gas-fluid flows, one phase persists in a scattered state, but in fluid-solid and gas-solid flows, the solid phase stays uniformly dispersed. Gathering experimental data is essential to comprehensively study the hydrodynamic characteristics of reactive flows that include both gas and solid particles. Yet, obtaining detailed experimental information presents challenges due to rigorous operating conditions and the expenses involved with measurement equipment. To address these constraints, computational fluid dynamics models, which are three-dimensional mathematical representations, have become an invaluable tool in this area of research. CFD models offer substantial contributions by enhancing current processes and enabling the advancement of new technologies. CFD results can provide valuable insights into real-world systems, offering both qualitative and frequently quantitative understandings that may not be feasible with experimental data. Precise simulation results are extremely beneficial in understanding and designing the dynamic functions of reactors. They offer extensive information about velocity and temperature patterns, turbulence in flow, The heat and mass transfer processes, along with reactions involving both solid and gas components. CFD simulations provide a range of advantages, including cost-effective analysis of the hydrodynamic performance in processes involving chemicals, systems of energy, and process applications for engineering. They also enhance and streamline process effectiveness, provide a way to see how systems behave in various operating scenarios, support analysis of potential risks and problem-solving in industrial facilities, reduce time and expenses when developing new designs, and make it easier to expand strategies. Computational fluid dynamics simulations offer a systematic and advanced method for comprehending intricate chemical and energy systems. Their capacity to provide numerical data, enhance effectiveness, assess potential hazards, and refine procedures renders them an essential asset in both academic research and industrial settings. Numerous numerical models can replicate the dynamic characteristics of reactive gas-solid flows within the contexts of energy systems and process engineering. The simplest approach, known as the mixture model, involves representing in contrast to homogenous gas-solid flow, a single-phase flow presupposes a uniform dispersion of particles in the fluid phase with negligible differences in velocities between the phases. By figuring out balancing equations, one may determine the physical characteristics of the fluid and solid phases, such as temperature, pressure, and velocity. Real flows deviate from these assumptions, so this approach suits only low solid content gas-solid flows.

4. CFD in Reactor study Two Fluid Model:

The analysis of gas-solid fluxes containing particles smaller than 1 mm is frequently performed using the two-phase model. It is mainly suitable for uniform gas-solid flows but can also be adapted to analyze diverse systems. An alternative way to handle varied systems is the multi-phase model. This expands the model of two-fluid that is encompass multiple particle phases and includes extra interplay components. It is extensively utilized in flows with three phases of gas, liquid, and solid, systems with different particle size distributions, and those with particles spread across a wide range. When considering changes in particle properties because of chemical reactions, considering each particle class or shape as an individual phase leads to increased computational demands. combining the momentum and continuity balance equations with the equation of the method of population balance in the two-fluid model enables the evolution of distinct particle properties over time to be modelled, rather than focusing on individual particles.

Multi-fluid approach and the fusion of two-fluid model with PBE (considering various particle sizes) could result in computational expenses comparable to those of the discrete-particle method. Currently, tracking several millions of particles within an acceptable range time frame makes demanding the DPM (Discrete-particle model). A fluidized bed gasifier system of 100 kg of evenly dispersed sand particles is simulated, each approximately 150 micrometers in diameter, entails the manipulation and computation of an astounding 22 billion individual particles. This magnitude far exceeds the operational capacity of present-day computers and even state-of-the-art high-performance clusters. Real-time simulations in 2004 were limited to managing about 10,000 particles because of communication constraints between the main memory and the CPU [19]. Since then, there have not been considerable boosts in processor clock speeds. However, transistor density has significantly increased while consuming less energy [20]. In today's context, it is feasible to simulate particle systems on the order of $O(10^6)$ using CPUs [21]. By utilizing graphical processing units, simulations can become notably faster and able to handle particle counts of up to 10^8 . However, these numbers are still insufficient for applications such as fluidized-bed simulations, even when conducted on a small scale in a laboratory. In a 24-hour period, Jajcevic et al. replicated 2.97 seconds of process time by simulating 1.7 million particles on a desktop GPU, while 25 million particles required 120 hours to replicate a single second of processing time [22]. In three frames per second, Govender et al. used a laptop with a GTX 880 GPU to build a spinning mill with 16 million particles. One billion particles might be handled by an NVIDIA K40 GPU with 12 GB of RAM at a time [23]. In a 2019 update, Xu et al. introduced a mixed Computing unit with CPU and GPU integration for modeling 3D full-loop circulating fluidized beds [24], simulating 1.27×10^{11} actual particles with 1.27×10^8 coarse-grained particles on 135 NVIDIA K80 GPUs. They achieved speeds of 1.5×10^7 updates for particles on each GPU in a second and set a benchmark for GPU-based discrete element method simulations [25]. To simulate gas-solid fluxes, a variety of commercial software programs, such as ANSYS FLUENT, BARRACUDA Virtual Reactor, and COMSOL Multiphysics, use models including mixture, two-fluid, discrete-particle, and hybrid models. These methods have shown successful in the research of particle fluidization [26][27][28]. A large number of the commercial CFD software and internally produced codes offer user-friendly interfaces with detailed models for gas-solid flows, encompassing flow, turbulence, thermodynamics, and heat transfer. These programs are in a continuous state of development and may not always provide specific details about their applications. These CFD programs, built by businesses and institutions, are frequently not publicly available.

5. Two Fluid Model:

The solid phase is seen as a thick secondary gas phase in the two-fluid concept, allowing both phases to be described using single-phase flow equations. Based on the premise that particles have properties comparable to those of gases, the KTGF determines transport parameters including granular pressure, viscosity, and stress [29]. Particles in motion display constant and unpredictable movement as they interact with the fluid medium in diluted systems or other particles/walls in coarse flows. After accounting for non-ideal particle-particle collisions and gas-particle drag, particles are able to move freely and interact with one another. Monitoring fluctuations in particle velocity, along with changes over time and position across computational space, is essential for establishing granular temperature. An analogous balance equation to the energy equation for fluid phases is used to represent this granular temperature. The essential equations of the two-fluid model in ANSYS FLUENT are easily expressed as follows: This model represents gas and solid phases as crossing continua within a mathematical framework, incorporating concepts like granular viscosity, pressure, and stress, which are modified by granular temperature. Below is a representation of the phase q mass conservation equation:

$$\frac{\partial}{\partial t}(\rho_q \varepsilon_q) + \nabla \cdot (\varepsilon_q \rho_q \vec{u}_q) = \sum_{p=1}^n (m_{pq} - m_{qp}) \dots \dots \dots 1$$

In this case, the sign ε_q signifies the volumetric fraction specific to phase q, denoting the proportion of space occupied by that particular phase. The term n denotes the number of phases present in the system. ρ_q and \vec{u}_q appropriately represent the phase q density as well as its velocity.

The following are the phase q momentum conservation equations:

$$\frac{\partial}{\partial t}(\rho_q \varepsilon_q \vec{u}_q) + \nabla \cdot \varepsilon_q \rho_q \vec{u}_q \vec{u}_q = \varepsilon_q \nabla \cdot T_q - \varepsilon_q \nabla p + \varepsilon_q (\vec{F}_{ext,q} + \vec{F}_{lift,q} + \vec{F}_{vm,q} + \vec{F}_{bas,q}) + \sum_{p=1}^n (\vec{R}_{pq} + m_{pq} \vec{u}_{pq} - m_{qp} \vec{u}_{qp}) \dots\dots\dots 2$$

The various forces per unit volume are denoted as follows: $\vec{F}_{ext,q}$ represents the external body force acting on phase q, $\vec{F}_{lift,q}$ denotes the Saffman force on phase q, $\vec{F}_{vm,q}$ stands for the virtual mass force on phase q, and $\vec{F}_{bas,q}$ represents the Basset force on phase q.

The term \vec{R}_{pq} , known as the drag force, refers to phase separation force as a function of phase volume. The interphase velocities are represented as \vec{u}_{pq} and \vec{u}_{qp} , which are determined based on the interphase mass transfer and can be interpreted as \vec{u}_q or \vec{u}_p as appropriate. For Newtonian fluids, the stress-strain tensor T_q can be determined using the following relationship:

$$T_q = \varepsilon_q \mu_s (\nabla \vec{u}_q + \nabla \vec{u}_q^T) + \varepsilon_q I_q \left(\lambda_q - \frac{2}{3} \mu_q \right) \nabla \cdot \vec{u}_q \dots\dots\dots 3$$

Where:

μ_q = dynamic viscosity

I_q = Unit matrix

T_q = fluid temperature

q represent the phase q

The secondary viscosity, often referred to as the volume viscosity or bulk viscosity, λ_q , can usually be ignored for incompressible fluids.

To achieve equilibrium in each phase, the specific enthalpy transport equation is solved. Subsequently, phase q temperature is determined by utilizing particular enthalpy and mean specific heat capacity:

$$\frac{\partial}{\partial t}(\rho_q \varepsilon_q h_q) + \nabla \cdot \varepsilon_q \rho_q \vec{u}_q h_q = \varepsilon_q \frac{\partial p}{\partial x} + \nabla \cdot \left(\frac{\rho_q \varepsilon_q}{Pr} \nabla h_q \right) + S_h \dots\dots\dots 4$$

For each component i, a substances of transport equation is additionally solved:

$$\frac{\partial}{\partial t}(\rho_q \varepsilon_q C_{q,i}) + \nabla \cdot \varepsilon_q \rho_q \vec{u}_q C_{q,i} = \nabla \cdot \left(\frac{\rho_q \varepsilon_q}{Pr} \nabla C_{q,i} \right) + S_h \dots\dots\dots 5$$

In the given context, p stands for the static pressure, and μ_q denotes the viscosity that varies with phase q. The Prandtl (Pr) and Schmidt (Sc) numbers are dimensionless number. The source term S_i considers the impact of chemical reactions on the creation or reduction of component i. Additionally, the heat source term S_h encompasses factors such as heat release from reactions, radiation contributions from phase q, heat transfer through convection, radiation, and mass transfer during the phase transition from phase p to phase q. Following the filtering process, the continuum equations remain unaltered; However, an extra term has been included in the momentum equations [30][31]. Studies by van der Hoef et al. [15] and Andrews et al. [32] have demonstrated that when the grid size is approximately ten times greater than the particle diameters, small-scale features become inconsequential in two-fluid model simulations. Consequently, detailed simulations require a very fine grid, which limits the domain size that can be simulated. Nevertheless, results from simulations within these smaller domains can subsequently guide two-fluid simulations on coarser grids by employing filtered two-fluid model equations. Several studies have highlighted that closure relations mainly depend on particle volumetric fraction and filter size [31], [32]. It has also been noted that outcomes differ from those of standard homogeneous two-fluid models and show reduced sensitivity to grid variations in filtered two-fluid models. Applying the Kinetic Theory of Granular Flow is necessary for the two-fluid model to effectively simulate concentrated gas-solid fluxes, which is limited in its ability to accommodate a specific range of variations in solid velocity compared to granular temperature. Gotz " and Kanther [33], [34] conducted studies and, respectively, The study looked at the Maxwell-Boltzmann distribution of particle velocities to determine the suitability of the two-fluid model for simulating dense gas-solid flows. Gotz " conducted a fluidized-bed simulation with an internal CFD/DEM code, enabling numerical calculation of particle velocity distribution. Significant departures from the anticipated Maxwell-Boltzmann distribution were noted in various regions of the obtained distributions. The most notable discrepancies were detected at the interface of gas bubbles and distributed solid particles within the fluidized bed. It is plausible that bimodal distribution functions may emerge in these boundary layers in future research which are not covered by existing KTGF framework. The impact

of these distribution functions on the precision of numerical simulations for dense gas-solid fluxes, however, is not well understood and may need more research.

Typically, the two-fluid model is employed for the flow of gas-solid that can be assuming the solid phase consists of uniform-sized of the particles (monodisperse). In scenarios where multiple phases of solid coexist, in fluidized-bed biomass gasifiers, which contain an inert sand bed and biomass, the two-fluid model must be expanded to incorporate the interactions between these separate solid phases. This extension is known as the MFM (multi-fluid model), which provides closure functions for each of the multiple solid phases, denoted here as s_n and s_m . Each of the solid phases, s_n and s_m , has a conservation equation that is constructed in a similar way, as shown in Eqs. 1, 2, 4, and 5. But momentum exchange between these solid phases requires another term to be taken into account in the MFM.:

$$\vec{R}_{nm} = K_{nm}(\vec{u}_{sn} - \vec{u}_{sm})$$

Syamlal et al. [35] presented the subsequent equation for computing the coefficient for solid-solid drag:

$$\beta_{nm}^{\text{Syamlal}} = \frac{3(1+e_{nm})\left(\frac{\pi}{2} + C_{fri,nm}\frac{\pi^2}{8}\right)\epsilon_{sn}\rho_{sn}\epsilon_{sm}\rho_{sm}(d_{sn}+d_{sm})^2 g_{nm}^{rad}}{2\pi(\rho_{sn}d_{sn}^3 + \rho_{sm}d_{sm}^3)}((\vec{u}_{sn} - \vec{u}_{sm})) \dots\dots\dots 6$$

The solid-solid drag coefficient ($\beta_{nm}^{\text{Syamlal}}$) is determined by several parameters, including the friction coefficient ($C_{fri,nm}$), the coefficient of restitution between solid phases (e_{nm}), the radial distribution function accounting for particle contacts between different solid phases (g_{nm}^{rad}), and the volumetric solid fractions of the respective solid phases (ϵ_{sn} and ϵ_{sm}). The radial distribution function between particles from various solid phases must be calculated using extensions of the equations found in the literature. For instance, one expression proposed by Iddir and Astratooopour [36] can be presented as follows:

$$g_{nm}^{rad} = \frac{1}{\left(1 - \frac{\epsilon_{sn}}{\epsilon_{sn,max}}\right)} + \frac{3}{2}d_{sn} \sum_{K=1}^M \frac{\epsilon_{sk}}{d_{sk}} \dots\dots\dots 7$$

Where

$$\epsilon_s = \sum_{K=1}^M \epsilon_{sk}$$

$$\epsilon_{s,max} = \sum_{k=1}^M \epsilon_{sk,max}$$

It is essential to recognize that in theory, there is no specific restriction on the quantity of solid phases (M) that can be incorporated into a simulation. Nevertheless, simulating granular flows with multiple solid phases can pose computational and technical challenges. As a result, for practical simulations, a simplified method is frequently utilized. In this situation, Particle interaction between distinct solid phases may be represented by the radial distribution function as:

$$g_{nm}^{rad} = \frac{d_{sn}g_{nm}^{rad} + d_{sm}g_{nm}^{rad}}{d_{sn} + d_{sm}} \dots\dots\dots 8$$

The multi-fluid model offers a versatile approach for effectively handling shifts in particle size distribution and changes in particle shape caused by chemical reactions. It particularly excels in situations involving systems with two or three distinct particle sizes. Gas-solid flows encountered in many engineering applications involve a wide range of particle sizes, leading to a complex particle size distribution. Consequently, as the number of solid phases being studied increases, the computational demand also substantially rises. Integrating the equation of population balance into the two-fluid model approach provides a comprehensive framework for handling complexities related to varying particle sizes in gas-solid flows by allowing for modeling both particle size distribution and the evolution of particles over time.

5.1. State of the art studies:

The biphasic paradigm has garnered extensive utilization across diverse domains of engineering, particularly within the realm of fluidized-bed systems. This segment furnishes an exhaustive retrospective analysis of the paradigm's evolution and subsequently delves into ongoing scholarly pursuits, commencing with non-reactive simulations and progressing toward publications centering on reactive simulations.

Owing to the copious array of literature concerning non-reactive simulations, this discourse predominantly leans upon review papers that chiefly scrutinize the evaluation of reactive simulations.

5.2. Current progress and research findings:

Anderson and Jackson's groundbreaking paper in 1967 laid the groundwork for the fundamental gas-solid flow equations of motion in a continuum context [37]. Ishii later expanded on this work in 1975 [38], deriving governing equations for multiphase fluid-fluid systems with some differences in underlying assumptions compared to Anderson and Jackson. The two-fluid model has since become a cornerstone for simulating various types of gas-solid flows, both reactive and non-reactive, including applications in fluidized bed systems. Lyczkowski's 2018 book [39] offers a detailed historical overview of the two-fluid model's gas-solid flow equations, intertwined with tales from the individual, highlighting his extensive collaboration with Gidaspow [40] over four decades. According to Lyczkowski's account, the roots of the two-fluid model can be traced back to 1966 when RELAPSE-1, a computer program was created to analyze incidents regarding the failure of nuclear reactors. In contrast to contemporary multiphase programs, RELAPSE-1 was quite simple, with just three nodes and it did not account for some physical phenomena and interactions as compared to the present programs. At that time, its computational approach more closely resembled a single-phase program using the mixture model [41], [42].

Solbrig and Hughes developed individual continuum equations for each phase in 1971 [43], which resulted in the creation of the SLOOP software. Unfortunately, this initiative faced obstacles and eventually stalled in 1975, partly because of computational difficulties linked to it. At that time, the SLOOP project members modified parts of the code to develop later computer programs like RELAP5, KACHINA, and K-FIX. In 1974 and 1975, F. Harlow and A. Amsden [44], [45], created the KACHINA code, which brought together earlier studies on this subject, standardizing language and settling disputes around phase interaction representation. They also carried out computerized examinations of particle movement through vapor. In the midst of the 1970s oil crisis, the US Department of Energy initiated efforts to enhance understanding of coal gasification hydrodynamics. However, these endeavors saw only partial success [46]. Then in the 1980s, there was the arrival of kinetic theory for granular flow which proposed using granular temperature for characterizing particle movement and calculating other factors such as solid pressure and viscosity. This idea became widely accepted after being discussed at several meetings beginning in 1986 [47]. Based on the K-FIX code, M. Syamlal began developing the MFIX code in 1985. He then incorporated the Multiparticle Non-Isothermal Fluidized Bed Program. The program's first release was made available in 1993. In 1995, FLUENT and NETL worked together to implement the multiphase code into the FLUENT platform through a joint R&D agreement. This led to the 1997 release of FLUENT, the first iteration including the two-fluid formulation. It is worth mentioning that ANSYS-FLUENT or MFIX is now used for simulations in a significant portion of the literature. Having said that, the two-fluid model is also viable in a wide variety of different CFD software, both free and paid. Examples include the 1978-created PHOENICS commercial code and the 2016-acquired Star-CCM+ code from Siemens, both of which were developed by D.B. Spalding [48]. In recent years, Open FOAM has become one of the most prominent open-source options for applications requiring the two-fluid model and the MFIX software [49]. A comprehensive literature search was conducted, spanning from 1991 to 2023, and almost one thousand papers pertaining to the two-fluid model were located. Nearly eighty percent of these articles focus on multiphase flow simulations without reactions. The simulations cover a wide variety of topics, including scaling up hydrodynamics, comparing 3D and 2D simulations, studying the transfer of heat phenomena, developing drag models, exploring KTGF, and using various turbulence models. Drag modeling has garnered substantial attention due to its major impact on the accuracy of multiphase flow forecasts. Conventional homogeneous drag models have a propensity to overestimate drag and may generate misleading results as they make the assumption that resistance and particle count in a cell are perfectly proportionate. However, in fluidized beds, particles often form smaller-than-cell clusters, which leads to lower resistance than predicted by homogeneous models. [50]. Scientists have established two fundamental methodologies, referred to as "fine-grid" and "coarse-grid" simulations, to address this problem. The "fine-grid" method entails refining the mesh until a solution independent of mesh size is achieved. The variable in the homogeneous drag model is altered using a correction factor in "coarse-grid" simulations. [51].

Another area of continuous investigation is the delivery of different particle sizes within the two-fluid model framework. For instance, in processes like catalytic changes such as FCC, solid particle properties (like size and density) maintain constant throughout time. Conversely, in non-catalytic processes like pyrolysis and polymerization, solid particle characteristics vary dependent on chemical reactions. One solution need constructing a fluid phase for each particle size, although this would result in greater processing time and perhaps numerical anomalies. Therefore, the population balance model was added into the two-fluid model to offer a more realistic description of the changing nature of solid particles via a population balance equation that describes their evolution from nucleation and growth to aggregation and fragmentation. [52]–[54].

5.3. Non-reactive simulation:

In the field of non-reactive simulation, a considerable body of published research has been reviewed, encompassing approximately 800 studies that were uncovered through thorough investigation. These studies primarily center on delving into gas-solid interactions (particularly drag modeling), examining hydrodynamics, and exploring mathematical elements associated with the two-fluid model (such as the advancement of kinetic theory in granular flow). Additionally, several studies have looked into whether two-dimensional (2D) and three-dimensional (3D) simulations yield comparable outcomes. This is a hotly debated topic in academic research.

5.4. Reactive simulation:

The two-phase model is used in a lot of different engineering fields for fluidized-bed systems. This paper summarizes recent studies based on the specific operations they simulate.

5.4.1. Pyrolysis, gasification, and combustion:

Thermal processes for converting solid fuel include combustion, gasification, and pyrolysis. Fluidized beds are often employed in these methods, with a considerable proportion of inert material that doesn't actively engage in the conversion reactions. This setup helps maintain consistent temperatures within the reactor even when there are abrupt fluctuations in fuel supply. These techniques also profit from efficient blending of gases and solids, enabling the use of solid fuels with different particle shapes, various sizes, and diverse energy contents. Further benefits can be highlighted as follows:

- Continuous operation with the ability to move solid materials into and out of the system without any breaks.
- The higher transfer rates of heat and mass from the gas phase to the solid phase lead to more uniform temperature distributions within the bed, even when undergoing highly exothermic or endothermic reactions.
- Operating flexibly across a diverse array of geometric and mechanical particle attributes.
- Outstanding blending capabilities.
- The capacity to utilize diverse solid fuels like coal, biomass, RDF, or fuel mixes. In addition, these technologies demonstrate substantially reduced NO_x and SO_2 content and providing for a safe, ecologically friendly, and sustainable energy source. Cost-effective operation compared to alternative technologies is an additional benefit that makes it suitable for large-scale use. Additionally, this technology has simple construction requirements leading low initial investments. Several studies have utilized the two-fluid model approach to investigate pyrolysis, gasification, and combustion processes in fluidized beds. Pyrolysis is a thermal process that breaks down organic materials without oxygen. It occurs at high temperatures above 250°C and doesn't involve interactions with oxygen, water, or other substances like hydrolysis and combustion do. However, it's important to note that some oxidation may occur during pyrolysis due to difficulties in creating an entirely oxygen-free environment. The term "pyrolysis" comes from the Greek words "pyro," meaning fire, and "lysis," meaning separation. Typically, pyrolysis is used to convert organic materials into solid residue containing ash and carbon as well as smaller amounts of liquids and gases [55]. During biomass pyrolysis, a multitude of chemicals are generated, such as char, tar, and gases like carbon monoxide, carbon dioxide, and nitrogen. Different chemicals are emitted at variable concentrations. Tar consists of thick hydrocarbons combined with organic acids, aldehydes, alcohols, and phenols. Over time, no decomposes into char, volatile components and fumes through subsequent processes.

The char that's produced is mostly carbon in solid form. The exact makeup of these primary components is influenced by factors like the type of biomass used, the oxidizing agent (like nitrogen, air or steam), how quickly heating happens, and how long the materials are heated. Pyrolysis, also called "torrefaction," happens between 200°C -400°C temperature range and takes around 15 to 90 minutes. This results in the release of water and low-calorific-value gaseous substances, leading to a roughly 1.3-fold increase in calorific value (by weight). Torrefied biomass shows improved properties compared to raw biomass, such as better grindability and reduced requirements for transportation and storage. In contrast, "carbonization" involves intense pyrolysis at elevated temperatures around 600°C with controlled oxygen presence for combustion-derived heat. This results in fixed carbon as the primary residue, yielding a denser solid fuel with higher energy content. However, it should be noted that carbonization has lower energy yield than torrefaction. The gasification method is employed to convert solid biomass fuel into a burnable gas-mixer, consisting mostly of hydrogen (H_2) and carbon monoxide, along with minor amounts of carbon dioxide, water vapor (H_2O), methane, nitrogen (N_2), and other hydrocarbons. This combination is commonly termed as producer gas [56]. Producer gas has numerous uses in power generation and as a raw material for valuable chemicals utilized in processes like Fischer-Tropsch synthesis, methanol manufacture, and ammonia synthesis. The process takes place at high temperatures above 500°C and needs regulated usage of gasifying substances such as oxygen, steam, or carbon dioxide without entirely burning the initial fuel source. Various carbon-based materials including biomass, coal, byproducts from petroleum like petcock, and industrial wastes can be appropriate fuel for this purpose. In the gasification process, pyrolysis begins the transformation by producing volatiles and char. The subsequent stages involve converting the char through gasification and reforming the volatiles through cracking. A significant drawback of traditional gasification is its dependence on pure oxygen as the agent for generating high-quality producer gas. Furthermore, effective gas cleaning is crucial and varies depending on specific end-use technology or compliance with emission standards, particularly focusing on eliminating gases such as CO_2 , hydrogen sulfide (H_2S), and carbonyl sulfide. Recent developments in gasification technology have brought about novel methods, new methods like chemical-looping gasification [57], [58], calcium-looping gasification [59], [60], dual fluidized bed gasifiers (indirect steam gasification) [61][62], solar-assisted gasification [63] using a dual fluidized bed [64], and indirectly irradiative fluidized-bed solar steam gasification. These up-and-coming approaches offer potential new options and improvements to traditional gasification methods. The process of combustion is a thermally favorable redox chemical reaction that involves the interaction between a fuel and an oxidant. It plays a crucial role as a primary source of heat in different uses, like combined-cycle and coal-fired thermal power plants, municipal waste incineration, and heat engines. These processes make use of the thermal energy produced by combustion while utilizing fuels in solid, liquid, or gaseous states [65]. When it comes to solid fuel combustion involving materials like coal, biomass, and municipal waste, the process becomes more complex with three essential drying, heating, and burning of gases and solid residue. The firebox of a steam generator or gas turbine typically produces flue gas containing mainly carbon dioxide, water vapor (H_2O), oxygen (O_2), nitrogen (N_2), sulfur dioxide, and argon. Recent advancements have brought about the oxy-fuel process as an alternative to traditional atmospheric air for capturing CO_2 emissions during combustion [66], [67]. Chemical-looping combustion has a variation termed oxygen-carrier-aided combustion, where instead of employing standard silica-sand bed material in fluidized bed combustion with air, metal oxide is employed [68]. The use of oxygen carriers as bed material increases the homogenous distribution of oxygen and temperature within the bed. This progress originates from a greater contact between fuel and air through a redox process, increasing the movement of oxygen from locations abundant in it to those deficient in order to promote effective burning. The chemical-looping process involves a dual fluidized-bed reactor configuration, with one unit as the combustor and the other as the air reactor.

5.4.2. Pyrolysis:

Depending on the kind of material used, such as biomass or coal, the pyrolysis processes in fluidized beds will take different forms. This assessment largely concentrates on biomass pyrolysis. Lathouwers and Bellan were pioneers in using the two-fluid idea for biomass pyrolysis in fluidized beds [69], [70]. This computational fluid dynamics model was applied to explore various operational conditions and scaling behavior.

Primary pyrolysis reactions (1-15)

Biomass $C_6H_{10}O_5$

42.27%wt
44.57%mol

30.93%wt
40.02%mol

18.10%wt
11.99%mol

1.61%wt
0.65%mol

7.08%wt
2.78%mol

Cell $C_6H_{10}O_5$

1 CellA

2 0.03%
5 H₂O
6 Char

3 88.86%

4 11.14%

1 LVG

0.16 CO₂
0.8 CO
0.9 H₂O
0.1 CH₄
0.2 Acetaldehyde
0.61 Char

0.95 HAA
0.25 Glyoxal
0.25 HMFU
0.2 Acetone

HCell $C_6H_{10}O_5$

5 40%

6 60%

7 41.68%

8 100%

1 Xylan

0.75 H₂
0.8 CO₂
1.4 CO
0.5 Formaldehyde
0.25 Methanol
0.125 Ethanol
0.125 H₂O
0.625 CH₄
0.25 C₂H₆
0.675 Char

1 CO₂
0.5 CH₄
0.25 C₂H₆
0.8 CO
0.8 H₂
0.7 CH₃O
0.25 Methanol
0.125 Ethanol
0.125 H₂O
1 Char

LignC $C_6H_{10}O_5$

9 100%

0.41 C₂H₆
1 H₂O
0.495 CH₄
1.32 CO
1 H₂
5.735 Char

0.1 p-Coumaryl
0.08 Phenol
0.35 LignCC

10 100%

0.7 H₂O
0.65 CH₄
0.6 C₂H₆
1 H₂
1.8 CO
6.4 Char

0.3 p-Coumaryl
0.2 Phenol
0.35 Acrylic-acid

LignH $C_6H_{10}O_5$

11 100%

1 Acetone
1 LignOH

12 100%

1 CO₂
1 LignOH

13 81.05%

14 39.79%

15 60.21%

1 Lumped-phenol

1 H₂O
2 CO
0.2 Formaldehyde
0.4 Methanol
0.2 Acetaldehyde
0.6 CH₄
0.65 C₂H₆
0.5 H₂
5.5 Char
0.2 Acetone

1 Lign

1 H₂O
2 CO
0.2 Formaldehyde
0.4 Methanol
0.2 Acetaldehyde
0.6 CH₄
0.65 C₂H₆
0.5 H₂
5.5 Char
0.2 Acetone

End product

Solid intermediate product

Tar subject to thermal cracking

Thermal cracking reactions (1-10)

HMFU	Acetone	p-Coumaryl	Phenol	Xylan	LVG	HAA	Glyoxal	Lumped-phenol	Acrylic-acid
1	2	3	4	5	6	7	8	9	10
3 CO 1.5 C ₂ H ₆	0.5 CO ₂ 0.5 H ₂ 1.25 C ₂ H ₆	1 CO ₂ 2.5 C ₂ H ₆ 3 Char	0.5 CO ₂ 1.5 C ₂ H ₆ 2.5 Char	2 CO ₂ 1 H ₂ 1.5 C ₂ H ₆	2.5 CO ₂ 1.5 H ₂ 1.75 C ₂ H ₆	2 CO 2 H ₂	2 CO 1 H ₂	2 CO ₂ 3 C ₂ H ₆ 3 Char	1 CO ₂ 1 C ₂ H ₆

78

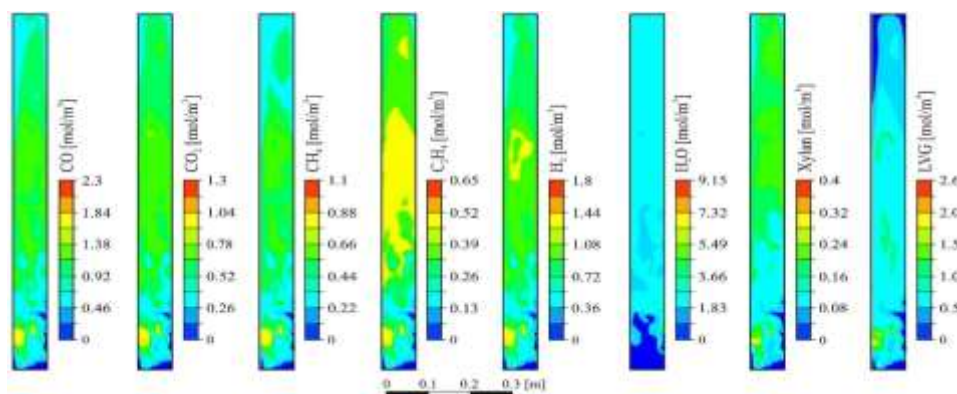


Fig 5: Distribution of species concentrations in a lab-scale fluidized-bed biomass pyrolyzer at $z= 0$ and 10.75 s

Furthermore, a team of researchers at Iowa State University built opensource application dubbed as BIOTC to simulate rapid biomass pyrolysis reactors [82]. Their inquiry comprises analyzing the impact of operating factors [83], interphase transfer processes [84], devolatilization methods [85], and fluid dynamics [86] employing the MFX platform. They also utilized a dispersed activation energy model concerning kinetic analysis [87]. Yan et al. [88] authenticated their computational hydrodynamics model using experimental evidence from Xue et al. and evaluated the influence of the fuel supply position on product output. In contrast, Lee et al. [89] employed a hybrid methodology of process simulation and CFD to maximize the effectiveness of a quick biomass pyrolysis reactor, covering both initial and final processes. They employed the Euler-Euler-Lagrange technique in MFX software to replicate several process scenarios, resulting to the construction of a yield data map for integrating CFD outputs into process simulation; nevertheless, they did not reveal detailed details on validating their CFD model. Ranganathan and Gu [90] carried out research in which they evaluated different kinetic models (basic [91], global [91], and advanced [92]) for high-speed pyrolysis reactors using ANSYS-FLUENT. They verified their computational fluid dynamics conclusions against actual experiments and discovered that the advanced model performed the most effectively. However, there was a mismatch of around 12% between the projected product yield and experimental results, specifically for non-condensable gases. Intriguingly, the computational fluid dynamics models did not validate the expected patterns in increasing particle size with the product yield. Sharma and colleagues [93] created a rudimentary kinetic framework [94] utilizing ANSYS-FLUENT to examine the influence of operational factors and particle size on fast biomass pyrolysis inside a fluidized bed. The verification of their computational fluid dynamics model was carried out against empirical data from Xue et al. [72]. The study concluded that the fluctuation of non-condensable gases could be related with ambiguities in tests. Aizi and Mowla [95] recreated A fluidized-bed reactor constructed particularly for the fast pyrolysis of algae, accomplished via the application of the MFX software. Their CFD results, especially concerning changing temperature patterns and mass flow rates, were confirmed through their own batch process testing. Lee and colleagues deployed [96] the MFX program to examine the impact of column dimensions on lignocellulose biomass pyrolysis in a fluidized bed. They applied a semi-global kinetic model and analyzed alternative column layouts with varying length-to-width ratios. However, they only validated the fluidization properties, particularly the lowest fluidization velocity, through experimental comparison. In another experiment, Eri et al. [97] evaluated the influence of potassium content on cellulose fast pyrolysis using ANSYS-FLUENT. They employed an updated reaction mechanism that integrated potassium's impact on kinetics [98]. Their computational fluid dynamics results correctly predicted experimental product yields with a 10% margin [98], [99]. Liu and colleagues [100] built a biomass pyrolysis model that comprised a comprehensive reaction system including cellulose, hemicellulose, and lignin. They employed a 3-parameter contraction model and the QMOM technique for their research (see Fig. 4). The study's numerical conclusions were contrasted with experimental data from varied biomass sources such as red oak, beechwood, and bagasse [99]. The accuracy of the modeling was revealed to significantly rely on the expected composition of the biomass.

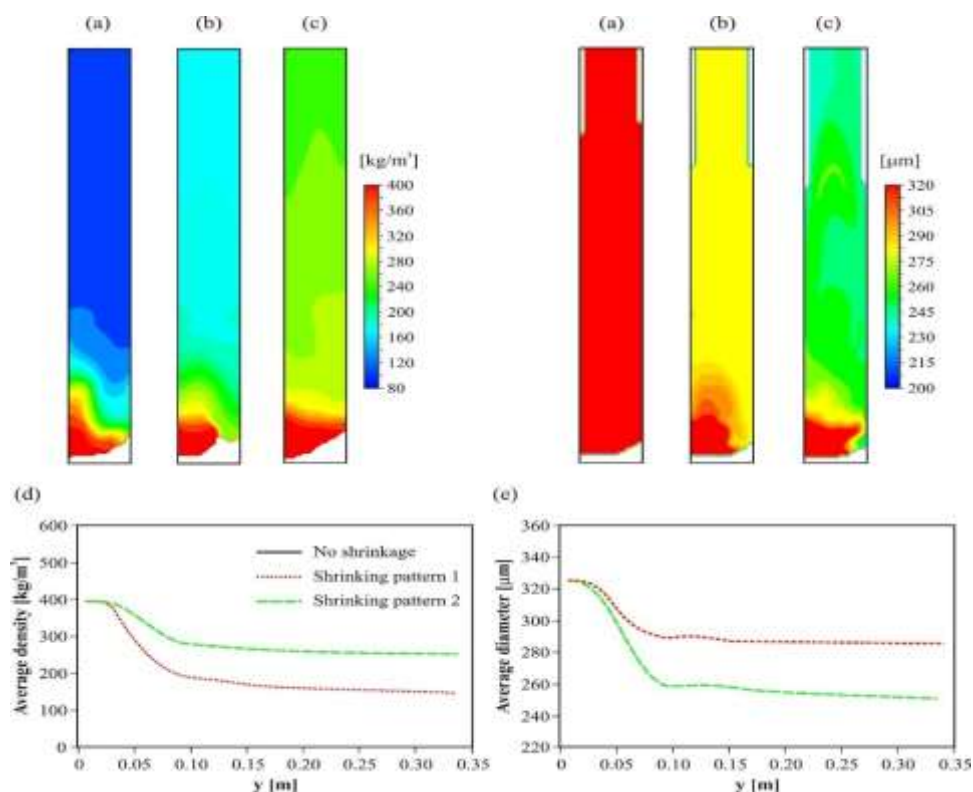


Fig 6: In a fluidized-bed pyrolyzer (marked as a, b, and c), the arrangement of biomass particles displays varied shrinkage patterns along the axis with regard to dimension (e) and apparent density (d): (a) No shrinkage, (b) Pattern 1, and (c) Pattern 2 [100].

Zhong and colleagues repeated rapid biomass pyrolysis tests done by Xue and others using ANSYS-FLUENT. Their inquiry contained various elements associated to particle transformation, such as particle diminution [101], [102], varied pyrolysis processes [103], and internal heat transmission similar to Dong et al.'s approaches [104]. Additionally, they employed a mix of EMMS and the Lu-Gidaspow drag model to face alterations in Geldart categorization within their simulations [105]. Most uses of the dual-liquid method or multi-fluid idea in thermal decomposition techniques have focused on rapid decomposition of organic waste in agitated fluidized beds. Variations in these ideas include variances in source materials, reaction rates, particle transformation models, and the CFD program employed. Different kinds of raw materials with diverse core elements (cellulose, hemicellulose, lignin) have been studied. many levels of intricacy regarding the basic components are revealed by numerous reaction mechanisms identified within scientific literature. Concerning the particle conversion model, modifications to a char and fresh biomass is catered for largely by adjustments to particle structures based on varying densities [106]. Recently, scientists have studied different approaches of particle reduction and some have effectively added a population equilibrium equation into the multi-fluid model design. The bulk of computational fluid dynamics models have been validated against tests carried out by Xue et al. [72] and Patel et al. [99], as well as against the experimentations done by other researchers [74]–[77], [95]. Substantial advancements have been achieved in CFD modeling of biomass rapid pyrolysis in fluidized beds, although there are still obstacles pertaining to precise forecasting of product yields, particularly for non-condensable gases, and comprehending the intricate physics associated with pyrolysis mechanisms. Papadikis et al. offered an alternate strategy known as the Euler-Euler-Lagrange method, contrasting it with the typical CFD-DEM methodology. In this methodology, the passive sand material is portrayed as an Eulerian phase, and individual active biomass particles are tracked as discrete components [107]–[110]. To model biomass rapid pyrolysis, a pyrolysis framework is implemented utilizing particular features in FLUENT 6.2 software. Additionally, the MFM has been employed to mimic various dynamic multiphase systems such as downer reactors [111], solar-thermal reactors [112], vortex reactors [113] and auger reactors [114].

5.4.3. Gasification:

In the milieu of gasification, fluidized-bed gasifiers commonly utilize biomass and coal as prevalent forms of feedstock. Numerous modeling facets, including the heat transfer, particle conversion and homogeneous reactions exhibit similarities for both types of feedstocks. Nevertheless, distinct modeling methodologies are necessary for heterogeneous reactions in this specific scenario.

5.5. Biomass Gasification:

Wang et al. use the sorghum biomass for gasification in fluidized bed [115] and employed a multi-fluid model and integrated a sophisticated kinetic model using their proprietary software, following the approach utilized by Lathouwers and Bellan to simulate pyrolysis [69], [70]. Nevertheless, they did not attempt a direct comparison with empirical findings.

Gerber and colleagues [116], originally from the Technical University of Berlin, employed the MFIX program in simulating a bubbling fluidized-bed wood gasifier. In their innovative procedure, they utilized char-coal as the bed material for their modeling. The simulation took into account three solid phases: wood particles having a diameter of 4 mm and two char stages with sizes of 1.5 mm and 2 mm, respectively. They compared two different two-step pyrolysis models, both derived from Grønli et al.'s [117] primary pyrolysis model but incorporating different secondary pyrolysis models – one including a single reactive tar component, and the other employing two reactive tar constituents featuring different reaction rate [118]. The data revealed that the pyrolysis model greatly altered the composition of generated gases. Although the numerical conclusions aligned well with those from tests by Neubauer and Behrendt [119], there was some variability regarding gas composition and temperature at the exit (Refers fig 5). Furthermore, the model exhibited difficulties in reproducing polydispersity and particle shrinkage, particularly due to its very basic approach to particle sizes and inability to account for segregation effects present in char particles.

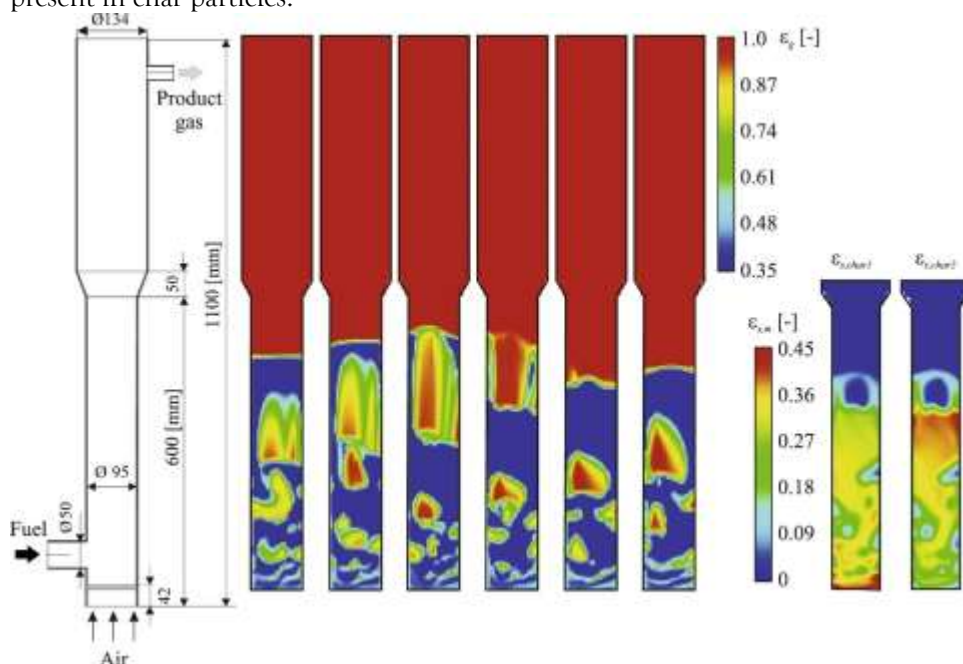


Fig 7: Experimental setup, gas phase volume fraction snapshots, and char volume fraction ($d_{char1} = 2$ mm, $d_{char2} = 1.5$ mm) associated with a experimental bubbling fluidized-bed biomass gasifier [116]. Chen and colleagues [120] carried out a study at Harbin University of Science and Technology, where they built an experimental fluidized-bed wood gasifier identical to the one used by Neubauer and Behrendt [119]. They adopted a computational fluid dynamics paradigm to the one used by Gerber et al. [116], but integrated a bubble-centric EMMS drag model put introduced by Shi et al. This adaption led to improved agreement with empirical data in contrast to adopting the Gidaspow drag model. He et al. employed ANSYS-FLUENT to model a small bubbling fluidized-bed wood gasifier [121], representing char and tar as empirical formulations of carbon, hydrogen, and oxygen, and basing yields on Wiest [122] and Rath and Staudinger's work [123]. Despite encompassing homogeneous and heterogeneous processes, the

model did not address kinetics directly. Their CFD findings, confirmed for varied equivalent and steam-to-biomass ratios, demonstrated consistency for H_2 generation but not for CO and CO_2 concentrations. Liu et al. created a 3D steady-state model utilizing a two-fluid technique to simulate a circulating fluidized-bed biomass gasifier [124], excluding transient components and comparing their model with experiments by Garcia-Ibanez et al. [125]. They found encouraging agreement for output gas concentrations but underestimated reactor temperature, further studying the impacts of turbulence models, radiation simulations, and the water-gas shift reaction. Xue and Fox [126] updated their CFD model in MFIX for wood gasification under pyrolysis, incorporating heterogeneous char and homogeneous reactions, and examining the effects of equivalent ratio, reactor temperature, and biomass moisture content, though their predicted biomass density changes could not be experimentally verified. Eri and colleagues [127] simulated the fluidized-bed gasification of pulverized almond shells using ANSYS-FLUENT with a multi-step multicomponent pyrolysis model similar to the one published by Mellin et al. [75]. Their model featured heterogeneous char reactions and homogeneous reactions. Despite utilizing an advanced pyrolysis model, their predicted findings differed significantly from experimental data published by Rapagna [128]. The expected tar content and char output surpassed the actual values by about 50%, while differences in gas composition ranged within 25% for H_2 and CO. Only the CO_2 and CH_4 fractions correlated well with the experimental results. In 2013, Couto and colleagues [129] reported the results of their investigations on coffee husk biomass gasification through testing and numerical simulations. Their two-dimensional computational fluid dynamics model, created using ANSYS-FLUENT, exhibited good agreement with the reported gas compositions at the gasifier output. Nevertheless, a detailed exposition of property allocation throughout the reactor covering volume fractions and species concentrations was noticeably lacking. It deserves highlighting that the authors stressed the vital necessity to broaden the CFD model's scope to encompass tar generation and more comprehensive devolatilization procedures. Couto et al. [129] expanded the CFD model in their following studies [130], [131] incorporating a devolatilization model published by Badzioch et al. [132], and adopting the finite-rate/eddy-dissipation model to handle homogeneous reactions with kinetics equivalent to those introduced by Yu et al. [133]. Furthermore, they added the kinetic/diffusion surface reaction model previously presented by Field, Baum, and Street [134], [135] for characterizing heterogeneous reactions into their framework. The inquiry encompassed nine unique experimental experiments, encompassing three varied kinds of biomass. Each kind of biomass got testing under three discrete operational parameters affecting reactor temperature and the proportion of biomass to air [130], [131]. Nevertheless, major effort was focused towards testing the gasification method using coffee husk. The outputs from the validation indicated an approximate mismatch of 20% between the anticipated compositions of producer gas and the empirical values found (refer to Figure 6).

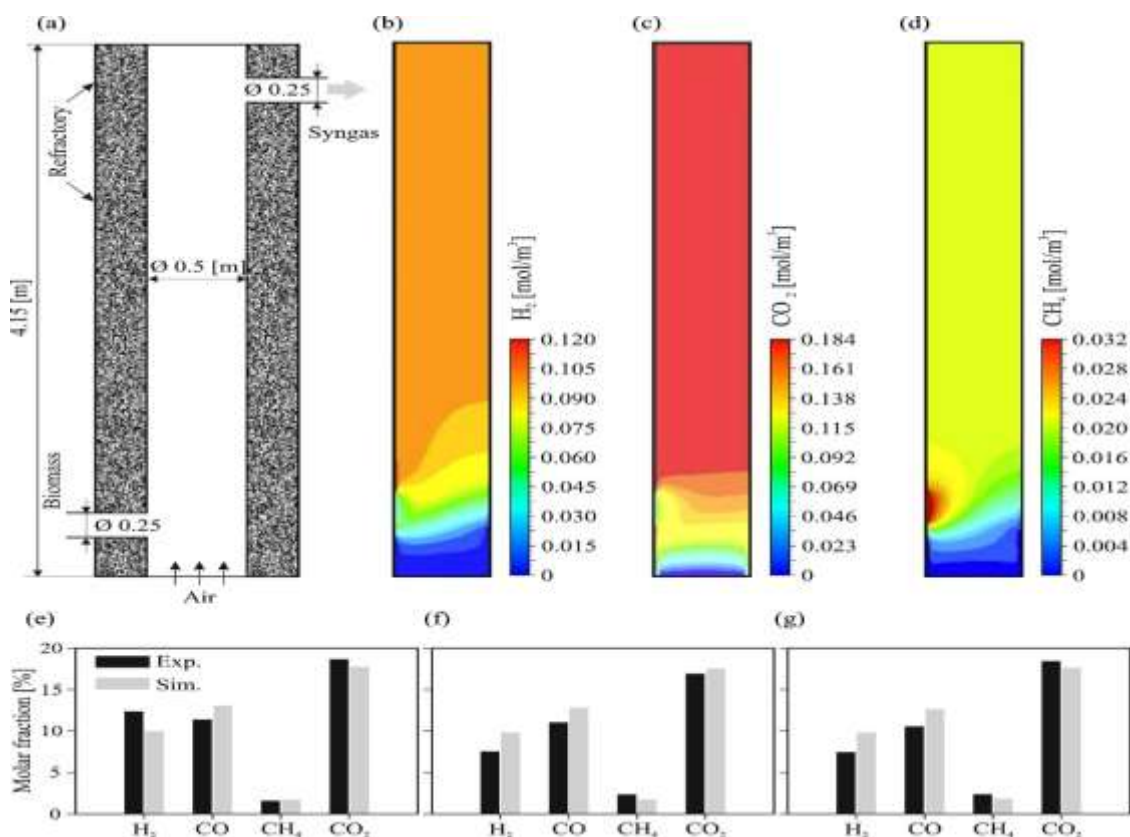


Fig 8: Three experimental runs with coffee husks were validated, and the outcomes were (a) gasifier geometry, (b, c, and d) distribution of gas molar fraction, and (e, f, and g) validation [136]

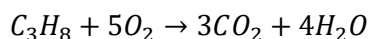
It is crucial to note that the actual particle size was not specified in either the experimental data or the computational fluid dynamics model. In their inquiry on the gasification of municipal solid waste, Couto et al. [137], [138] employed the aforementioned CFD model enhanced with an improved pyrolysis model to add secondary tar formation [139]. The experimental results by Wang et al. served as the basis for their computations [140]. While the CFD model demonstrated high agreement across most operating scenarios, differences of up to 40% were detected in certain gas components, especially hydrocarbons like CH_4 and C_2H_4 . These differences could likely be attributable to limited understanding of garbage composition and behavior. The confirmed Computational Fluid Dynamics model was utilized to examine the pilot-scale gasifier employing Municipal Solid Waste from Portugal under various process variables, encompassing reactor temperature, fuel feed rates, and air feed rate. The researchers also broadened the application of the CFD model to simulate the gasification of MSWs and other biomass sources utilizing CO_2 [141] and steam [142][137] as gasification agents [143]. Furthermore, miscanthus gasification was integrated into the enlarged CFD model. Notwithstanding correctly capturing overall patterns for a range of comparable ratios, it continuously inflated CH_4 concentration in all situations. Ismail and his co-authors [144], [145] additionally applied their own software, dubbed as combustion mathematics, and investigated energy transfer in order to model the pilot-scale fluidized-bed gasifier. Computational Fluid Dynamics findings for different feedstocks, including coffee husks [146], peach stones [145], [147], and miscanthus [143], were comprehensively confirmed against a range of experimental gasifiers [130], [131], [148], [149]. Additionally, several other research efforts relevant to the CFD model were done. These included a comparison between zero-dimensional technique and CFD [150], an evaluation of scale-up implications [151], and the merging of CFD with the Response Surface approach [152], [153].

5.6. Combustion:

A detailed investigation by Chalermssinsuwan et al. [154] explored three unique riser designs: tapered-in, tapered-out, and non-tapered configurations, seeking to analyze chemical processes and confirm the computer model using empirical data. Using a two-dimensional computational domain of 14.2 meters in height and 0.2 meters in diameter, split into 5,415 cells, simulations were done using ANSYS-FLUENT

software. Initial validation using cold flow simulations demonstrated significant agreement with empirical data from Particulate Solid Research Inc., notably in the spatial distribution of solid density at a height of 3.9 meters inside the riser. This was followed by researching reactive components to discover how riser geometry effects chemical reactions.

A simplified propane combustion reaction served as the focal point for this investigation.



With the reaction rate:

$$r = -ke^{\frac{E_a}{RT}} C_{C_3H_8} C_{O_2}^5$$

Utilizing quintet activation levels provided illumination into the influence of riser shapes on chemical reactions. The findings indicated that conical-inward risers were appropriate for reactions with sluggish kinetics, while conical-outward risers were advantageous for rapid reaction kinetics. Standard riser geometry produced favorable results for intermediate reaction kinetics. Concurrently, Southeast University has conducted an array of research articles delving into aspects of coal combustion in fluidized beds, enriching our understanding of the complex mechanisms inherent in these systems. Similarly, Zhou et al. [155] employed five activation levels to explore combustion in fluidized beds with different riser shapes, finding that tapered-in risers suited slow reactions, tapered-out risers suited rapid reactions, and conventional risers were ideal for intermediate rates. Fig 7 (a) shows the test rig geometry. Subsequent investigations by Zhou et al. [156], [157] extended on this by exploring nitrogen and sulfur emissions, and oxy-fuel combustion, establishing solid model agreements with empirical data and important discoveries on CO₂ concentrations and emission estimates[158]. Fig 7 (b) shows the comparison of experimental data of outlet gas composition and temperature gradients at different height and fig 7 (c) shows the simulated concentration of NO and SO_x with experimental data. Wu et al. [159] [160] [161] also performed comprehensive coal combustion testing in fluidized beds, establishing exact predictions of critical parameters and improving the knowledge of oxy-fuel combustion. Vepsäläinen et al. [162], [163] concentrated on interphase mass transfer in fluidized-bed combustion, estimating Sherwood numbers and mass transfer coefficients for various particle kinds with great precision. Myöhänen et al. [164] studied oxy-fuel combustion in a full-scale CFB power plant, revealing minor alterations were required for current designs to sustain combustion temperatures. Nikolopoulos et al. [165] effectively simulated NO_x and N₂O generation in lignite combustion, confirming their technique with lower computing costs. Soria et al. [166] explored heavy metal vaporization in incinerators, establishing exact estimates utilizing a two-fluid model framework. Li et al. [167], [168] and fryer and potter [169] created a model for chemical processes in fluidized beds, exhibiting the fluctuation of Schmidt numbers and attaining remarkable concordance with experimental data.

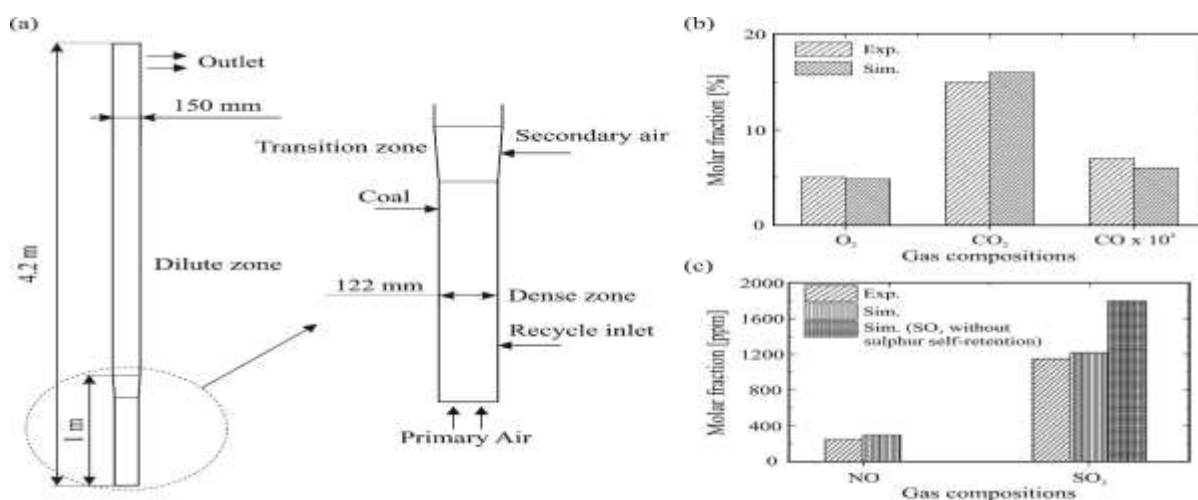


Fig 9: (a) The CFB riser's design, (b) the gas composition at the exit (both in modeling and experiment), and (c) the concentrations of nitrogen and sulfur oxide emissions, both in simulation and measurement [155][156]

Xu et al. [170] and Ji et al. [171] simulated sodium transformation in supercritical CFB boilers, getting respectable results in key parameters while greatly lowering computing time. Fig 8 shows that the simulated and measured gaseous temperature profile.

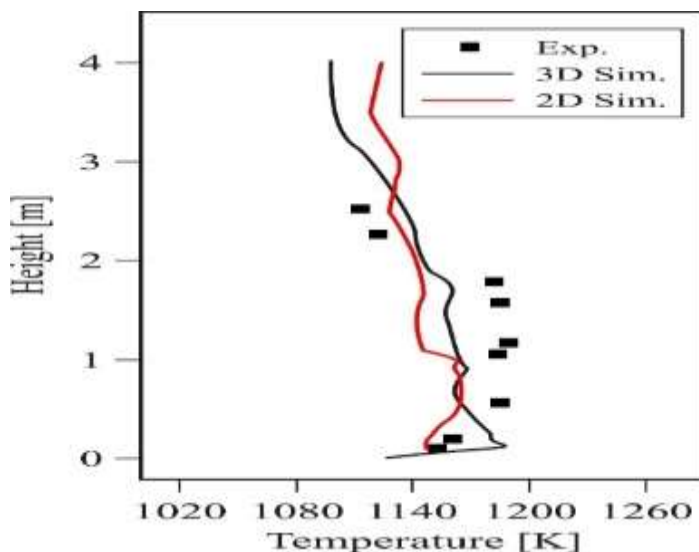


Fig 10: Experimental and simulated gas temperature [171]

Analysis revealed higher temperatures correlated with increased rates of sodium emissions resulting in diminished NaCl concentrations and Na₂SO₄; however, these elevated temperatures led to greater deposits of sodium and ash on heat transfer surfaces amid aligning well with experimental data.

6. CONCLUSION:

The research presented in this paper underscores the significant strides made in utilizing the two-fluid model for CFD simulations in fluidized bed gasifiers. By incorporating advanced sub-models and experimental validation, researchers have enhanced the accuracy and reliability of simulations, shedding light on complex processes such as devolatilization, heterogeneous reactions, and species concentrations. The findings emphasize the potential of CFD simulations in optimizing reactor design, improving heat and mass transfer processes, and advancing our understanding of fluidized bed systems. Looking ahead, continued research efforts to refine the two-fluid model and integrate multi-scale simulation methods hold promise for further advancements in industrial applications, emission control, and efficiency optimization in fluidized bed processes.

7. FUTURE DIRECTION:

Moving forward, further research in this field could explore the integration of artificial intelligence and machine learning techniques to enhance the predictive accuracy of CFD simulations in fluidized bed gasifiers. By leveraging big data analytics and advanced algorithms, researchers can develop more sophisticated models that capture the complex dynamics of gas-solid interactions with higher precision. Additionally, investigating the potential of coupling CFD simulations with process optimization algorithms could lead to real-time control strategies for fluidized bed systems, enabling dynamic adjustments to reactor conditions for optimal performance. Furthermore, exploring the incorporation of renewable energy sources and novel reactor designs in conjunction with CFD simulations could pave the way for sustainable energy solutions with reduced environmental impact. Overall, the future of research in this area holds immense potential for revolutionizing fluidized bed technology and advancing towards a greener and more efficient energy landscape.

REFERENCES:

- [1] A. Khosla et al., "Emergence of MXene and MXene-Polymer Hybrid Membranes as Future- Environmental Remediation Strategies," *Adv. Sci.*, vol. 9, no. 36, pp. 1-43, 2022, doi: 10.1002/advs.202203527.
- [2] B. Hare, N. Hühne, J. Gütschow, M. Schaeffer, and M. Vieweg-Mersmann, "Climate Action Tracker." 2015.

- [3] N. I. Khan, F. Elahi, and M. A. R. Rana, "A study on the effects of global warming in Bangladesh," *Int. J. Environ. Monit. Anal.*, vol. 3, no. 3, pp. 118–121, 2015.
- [4] J. T. Fasullo, B. L. Otto-Bliesner, and S. Stevenson, "ENSO's changing influence on temperature, precipitation, and wildfire in a warming climate," *Geophys. Res. Lett.*, vol. 45, no. 17, pp. 9216–9225, 2018.
- [5] energy institute, "Statistical Review of World Energy," 2023.
- [6] D. Geldart, "Types of gas fluidization," *Powder Technol.*, vol. 7, no. 5, pp. 285–292, 1973.
- [7] W. Kong, T. Tan, J. Baeyens, G. Flamant, and H. Zhang, "Bubbling and slugging of geldart group A powders in small diameter columns," *Ind. Eng. Chem. Res.*, vol. 56, no. 14, pp. 4136–4144, 2017.
- [8] H. L. Zhang, J. Degève, R. Dewil, and J. Baeyens, "Operation diagram of circulating fluidized beds (CFBs)," *Procedia Eng.*, vol. 102, pp. 1092–1103, 2015.
- [9] L. Reh, "Fluidized bed processing," *Chem. Eng. Prog.*, vol. 67, no. 2, p. 58, 1971.
- [10] J. R. Grace, "Contacting modes and behaviour classification of gas–solid and other two-phase suspensions," *Can. J. Chem. Eng.*, vol. 64, no. 3, pp. 353–363, 1986.
- [11] D. Kunii and O. Levenspiel, *Fluidization engineering*. Butterworth-Heinemann, 1991.
- [12] N. G. Deen, M. V. S. Annaland, M. A. Van der Hoef, and J. A. M. Kuipers, "Review of discrete particle modeling of fluidized beds," *Chem. Eng. Sci.*, vol. 62, no. 1–2, pp. 28–44, 2007.
- [13] M. A. van der Hoef, M. van Sint Annaland, and J. A. M. Kuipers, "Computational fluid dynamics for dense gas–solid fluidized beds: a multi-scale modeling strategy," *Chem. Eng. Sci.*, vol. 59, no. 22–23, pp. 5157–5165, 2004.
- [14] Y. Tsuji, "Multi-scale modeling of dense phase gas–particle flow," *Chem. Eng. Sci.*, vol. 62, no. 13, pp. 3410–3418, 2007.
- [15] M. A. van der Hoef, M. Ye, M. van Sint Annaland, A. T. Andrews, S. Sundaresan, and J. A. M. Kuipers, "Multiscale modeling of gas-fluidized beds," *Adv. Chem. Eng.*, vol. 31, pp. 65–149, 2006.
- [16] E. Loth *et al.*, "13.1 Overview of Multiphase Modeling." *Multiphase Flow Handbook*: CRC press, 2006.
- [17] M. Kuerten, "JG (2016). Point-Particle DNS and LES of Particle-Laden Turbulent flow-a state-of-the-art review," *Flow, Turbul. Combust.*, vol. 97, no. 3, p. 689.
- [18] F. Alobaid and F. Alobaid, "Computational fluid dynamics," *Numer. Simul. Next Gener. Therm. Power Plants*, pp. 87–204, 2018.
- [19] A. Kolb, L. Latta, and C. Rezk-Salama, "Hardware-based simulation and collision detection for large particle systems," *Proc. SIGGRAPH/Eurographics Work. Graph. Hardw.*, pp. 123–132, 2004, doi: 10.1145/1058129.1058147.
- [20] A. Danowitz, K. Kelley, J. Mao, J. P. Stevenson, and M. Horowitz, "CPU DB: recording microprocessor history," *Commun. ACM*, vol. 55, no. 4, pp. 55–63, 2012.
- [21] S. Yang, K. Luo, K. Zhang, K. Qiu, and J. Fan, "Numerical study of a lab-scale double slot-rectangular spouted bed with the parallel CFD–DEM coupling approach," *Powder Technol.*, vol. 272, pp. 85–99, 2015.
- [22] D. Jajcevic, E. Siegmann, C. Radeke, and J. G. Khinast, "Large-scale CFD–DEM simulations of fluidized granular systems," *Chem. Eng. Sci.*, vol. 98, pp. 298–310, 2013.
- [23] N. Govender, R. K. Rajamani, S. Kok, and D. N. Wilke, "Discrete element simulation of mill charge in 3D using the BLAZE-DEM GPU framework," *Miner. Eng.*, vol. 79, pp. 152–168, 2015.
- [24] J. Xu, X. Liu, S. Hu, and W. Ge, "Virtual process engineering on a three-dimensional circulating fluidized bed with multiscale parallel computation," *J. Adv. Manuf. Process.*, vol. 1, no. 1–2, p. e10014, 2019.
- [25] L. Lu *et al.*, "Computer virtual experiment on fluidized beds using a coarse-grained discrete particle method–EMMS-DPM," *Chem. Eng. Sci.*, vol. 155, pp. 314–337, 2016.
- [26] A. Stroh, F. Alobaid, M. T. Hasenzahl, J. Hilz, J. Ströhle, and B. Eppele, "Comparison of three different CFD methods for dense fluidized beds and validation by a cold flow experiment," *Particuology*, vol. 29, pp. 34–47, 2016.
- [27] A. Klimanek and J. Bigda, "CFD modelling of CO₂ enhanced gasification of coal in a pressurized circulating fluidized bed reactor," *Energy*, vol. 160, pp. 710–719, 2018.
- [28] C. M. Venier, A. Reyes Urrutia, J. P. Capossio, J. Baeyens, and G. Mazza, "Comparing ANSYS Fluent® and OpenFOAM® simulations of Geldart A, B and D bubbling fluidized bed hydrodynamics," *Int. J. Numer. Methods Heat Fluid Flow*, vol. 30, no. 1, pp. 93–118, 2020.
- [29] S. Chapman and T. G. Cowling, *The mathematical theory of non-uniform gases: an account of the kinetic theory of viscosity, thermal conduction and diffusion in gases*. Cambridge university press, 1990.
- [30] D. Z. Zhang and W. B. VanderHeyden, "The effects of mesoscale structures on the macroscopic momentum equations for two-phase flows," *Int. J. Multiph. Flow*, vol. 28, no. 5, pp. 805–822, 2002, doi: 10.1016/S0301-9322(02)00005-8.
- [31] Z. Qiao, Z. Wang, C. Zhang, S. Yuan, Y. Zhu, and J. Wang, "PVAm-PIP/PS composite membrane with high performance for CO₂/N₂ separation," *AIChE J.*, vol. 59, no. 4, pp. 215–228, 2012, doi: 10.1002/aic.
- [32] A. T. Andrews IV, P. N. Loezos, and S. Sundaresan, "Coarse-grid simulation of gas-particle flows in vertical risers," *Ind. Eng. Chem. Res.*, vol. 44, no. 16, pp. 6022–6037, 2005, doi: 10.1021/ie0492193.
- [33] S. Götz, *Gekoppelte CFD/DEM-simulation blasenbildender wirbelschichten*. Shaker, 2006.
- [34] W. Kanther, *Gas-Feststoff-Strömungen in komplexen Geometrien*. Shaker, 2003.
- [35] M. Syamlal, W. Rogers, and T. J. O'Brien, "MFIx documentation theory guide," USDOE Morgantown Energy Technology Center, WV (United States), 1993.
- [36] H. Iddir and H. Arastoopour, "Modeling of multitype particle flow using the kinetic theory approach," *AIChE J.*, vol. 51, no. 6, pp. 1620–1632, 2005.
- [37] T. B. Anderson and R. Jackson, "Fluid mechanical description of fluidized beds. Equations of motion," *Ind. Eng. Chem. Fundam.*, vol. 6, no. 4, pp. 527–539, 1967.

- [38] M. Ishii, "Thermo-fluid dynamic theory of two-phase flow," *NASA Sti/recon Tech. Rep. A*, vol. 75, p. 29657, 1975.
- [39] R. W. Lyczkowski, *The History of Multiphase Science and Computational Fluid Dynamics: A Personal Memoir*. Springer, 2017.
- [40] D. Gidaspow, *Multiphase flow and fluidization: continuum and kinetic theory descriptions*. Academic press, 1994.
- [41] G. L. Mesina, "A history of RELAP computer codes," *Nucl. Sci. Eng.*, vol. 182, no. 1, pp. v-ix, 2016.
- [42] K. V Moore and W. H. Rettig, "RELAP2: A DIGITAL PROGRAM FOR REACTOR BLOWDOWN AND POWER EXCURSION ANALYSIS," Phillips Petroleum Co., Idaho Falls, Idaho. Atomic Energy Div., 1968.
- [43] C. Solbrig and E. D. Hughes, "Two phase flow equations which account for unequal phase velocities and unequal phase temperatures," Idaho National Lab.(INL), Idaho Falls, ID (United States), 1971.
- [44] F. H. Harlow and A. A. Amsden, "Numerical calculation of multiphase fluid flow," *J. Comput. Phys.*, vol. 17, no. 1, pp. 19-52, 1975.
- [45] A. A. Amsden and F. H. Harlow, "KACHINA: An Eulerian computer program for multifield fluid flows," Los Alamos National Lab.(LANL), Los Alamos, NM (United States), 1974.
- [46] T. R. Blake, *Computer modeling of coal gasification reactors*. Department of Energy, 1976.
- [47] D. Gidaspow, J. Jung, and R. K. Singh, "Hydrodynamics of fluidization using kinetic theory: an emerging paradigm: 2002 Flour-Daniel lecture," *Powder Technol.*, vol. 148, no. 2-3, pp. 123-141, 2004.
- [48] A. K. Runchal, "Brian spalding: CFD & reality: A personal recollection," *J. Franklin Inst.*, vol. 351, no. 1, pp. 65-87, 2014.
- [49] C. J. Greenshields, "OpenFOAM user guide," *OpenFOAM Found. Ltd, version*, vol. 3, no. 1, p. 47, 2015.
- [50] K. Hong, W. Wang, Q. Zhou, J. Wang, and J. Li, "An EMMS-based multi-fluid model (EFM) for heterogeneous gas-solid riser flows: Part I. Formulation of structure-dependent conservation equations," *Chem. Eng. Sci.*, vol. 75, pp. 376-389, 2012.
- [51] W. Wang, B. Lu, N. Zhang, Z. Shi, and J. Li, "A review of multiscale CFD for gas-solid CFB modeling," *Int. J. Multiph. Flow*, vol. 36, no. 2, pp. 109-118, 2010.
- [52] H. A. Jakobsen, "Chemical reactor modeling," *Multiph. React. Flows*, 2008.
- [53] D. Ramkrishna, *Population balances: Theory and applications to particulate systems in engineering*. Elsevier, 2000.
- [54] X. Chen, J. Wang, and J. Li, "Coarse grid simulation of heterogeneous gas-solid flow in a CFB riser with polydisperse particles," *Chem. Eng. J.*, vol. 234, pp. 173-183, 2013.
- [55] A. Sharma, V. Pareek, and D. Zhang, "Biomass pyrolysis—A review of modelling, process parameters and catalytic studies," *Renew. Sustain. energy Rev.*, vol. 50, pp. 1081-1096, 2015.
- [56] S. K. Sansaniwal, K. Pal, M. A. Rosen, and S. K. Tyagi, "Recent advances in the development of biomass gasification technology: a comprehensive review," *Renew Sustain Energy Rev*, vol. 72, 2017, doi: 10.1016/j.rser.2017.01.038.
- [57] P. Dieringer, F. Marx, F. Alobaid, J. Ströhle, and B. Eppe, "Process control strategies in chemical looping gasification—A novel process for the production of biofuels allowing for net negative CO₂ emissions," *Appl. Sci.*, vol. 10, no. 12, p. 4271, 2020.
- [58] J. Zeng, R. Xiao, H. Zhang, Y. Wang, D. Zeng, and Z. Ma, "Chemical looping pyrolysis-gasification of biomass for high H₂/CO syngas production," *Fuel Process. Technol.*, vol. 168, pp. 116-122, 2017.
- [59] S. Chen, D. Wang, Z. Xue, X. Sun, and W. Xiang, "Calcium looping gasification for high-concentration hydrogen production with CO₂ capture in a novel compact fluidized bed: simulation and operation requirements," *Int. J. Hydrogen Energy*, vol. 36, no. 8, pp. 4887-4899, 2011.
- [60] M. Beirrow, A. M. Parvez, M. Schmid, and G. Scheffknecht, "A detailed one-dimensional hydrodynamic and kinetic model for sorption enhanced gasification," *Appl. Sci.*, vol. 10, no. 17, p. 6136, 2020.
- [61] K. Myöhänen, J. Palonen, and T. Hyppänen, "Modelling of indirect steam gasification in circulating fluidized bed reactors," *Fuel Process. Technol.*, vol. 171, pp. 10-19, 2018.
- [62] J. Karl and T. Pröll, "Steam gasification of biomass in dual fluidized bed gasifiers: A review," *Renew. Sustain. Energy Rev.*, vol. 98, pp. 64-78, Dec. 2018, doi: 10.1016/J.RSER.2018.09.010.
- [63] X. Li et al., "Hydrogen production of solar-driven steam gasification of sewage sludge in an indirectly irradiated fluidized-bed reactor," *Appl. Energy*, vol. 261, p. 114229, 2020.
- [64] M. Suárez-Almeida, A. Gómez-Barea, A. F. Ghoniem, and C. Pfeifer, "Solar gasification of biomass in a dual fluidized bed," *Chem. Eng. J.*, vol. 406, p. 126665, 2021.
- [65] H. Spliethoff, *Power generation from solid fuels*. springer science & business media, 2010.
- [66] J. Adánez, A. Abad, T. Mendiara, P. Gayán, L. F. De Diego, and F. García-Labiano, "Chemical looping combustion of solid fuels," *Prog. Energy Combust. Sci.*, vol. 65, pp. 6-66, 2018.
- [67] A. Abad, T. Mattisson, A. Lyngfelt, and M. Rydén, "Chemical-looping combustion in a 300 W continuously operating reactor system using a manganese-based oxygen carrier," *Fuel*, vol. 85, no. 9, pp. 1174-1185, 2006.
- [68] H. Thunman, F. Lind, C. Bretholtz, N. Berguerand, and M. Seemann, "Using an oxygen-carrier as bed material for combustion of biomass in a 12-MWth circulating fluidized-bed boiler," *Fuel*, vol. 113, pp. 300-309, 2013.
- [69] D. Lathouwers and J. Bellan, "Yield optimization and scaling of fluidized beds for tar production from biomass," *Energy & Fuels*, vol. 15, no. 5, pp. 1247-1262, 2001.
- [70] D. Lathouwers and J. Bellan, "Modeling of dense gas-solid reactive mixtures applied to biomass pyrolysis in a fluidized bed," *Int. J. Multiph. Flow*, vol. 27, no. 12, pp. 2155-2187, 2001.
- [71] Q. Xue, T. J. Heindel, and R. O. Fox, "A CFD model for biomass fast pyrolysis in fluidized-bed reactors," *Chem. Eng. Sci.*, vol. 66, no. 11, pp. 2440-2452, 2011.
- [72] Q. Xue, D. Dalluge, T. J. Heindel, R. O. Fox, and R. C. Brown, "Experimental validation and CFD modeling study of

- biomass fast pyrolysis in fluidized-bed reactors," *Fuel*, vol. 97, pp. 757–769, 2012.
- [73] Q. Xue and R. O. Fox, "Computational modeling of biomass thermochemical conversion in fluidized beds: particle density variation and size distribution," *Ind. Eng. Chem. Res.*, vol. 54, no. 16, pp. 4084–4094, 2015.
- [74] A. A. Boateng and P. L. Mtui, "CFD modeling of space-time evolution of fast pyrolysis products in a bench-scale fluidized-bed reactor," *Appl. Therm. Eng.*, vol. 33, pp. 190–198, 2012.
- [75] P. Mellin, E. Kantarelis, and W. Yang, "Computational fluid dynamics modeling of biomass fast pyrolysis in a fluidized bed reactor, using a comprehensive chemistry scheme," *Fuel*, vol. 117, pp. 704–715, 2014.
- [76] P. Mellin, Q. Zhang, E. Kantarelis, and W. Yang, "An Euler–Euler approach to modeling biomass fast pyrolysis in fluidized-bed reactors–Focusing on the gas phase," *Appl. Therm. Eng.*, vol. 58, no. 1–2, pp. 344–353, 2013.
- [77] P. Mellin, E. Kantarelis, C. Zhou, and W. Yang, "Simulation of bed dynamics and primary products from fast pyrolysis of biomass: steam compared to nitrogen as a fluidizing agent," *Ind. Eng. Chem. Res.*, vol. 53, no. 30, pp. 12129–12142, 2014.
- [78] B. Hejazi, J. R. Grace, X. Bi, and A. Mahecha-Botero, "Kinetic model of steam gasification of biomass in a bubbling fluidized bed reactor," *Energy & Fuels*, vol. 31, no. 2, pp. 1702–1711, 2017.
- [79] B. Hejazi, J. R. Grace, X. Bi, and A. Mahecha-Botero, "Kinetic model of steam gasification of biomass in a dual fluidized bed reactor: Comparison with pilot-plant experimental results," *Energy & Fuels*, vol. 31, no. 11, pp. 12141–12155, 2017.
- [80] A. Fernandez, C. Palacios, M. Echegaray, G. Mazza, and R. Rodriguez, "Pyrolysis and combustion of regional agro-industrial wastes: thermal behavior and kinetic parameters comparison," *Combust. Sci. Technol.*, vol. 190, no. 1, pp. 114–135, 2018.
- [81] K. Zeng, D. Gauthier, J. Soria, G. Mazza, and G. Flamant, "Solar pyrolysis of carbonaceous feedstocks: A review," *Sol. Energy*, vol. 156, pp. 73–92, 2017.
- [82] Q. Xiong, S. Aramideh, A. Passalacqua, and S.-C. Kong, "BIOTC: an open-source CFD code for simulating biomass fast pyrolysis," *Comput. Phys. Commun.*, vol. 185, no. 6, pp. 1739–1746, 2014.
- [83] Q. Xiong, S. Aramideh, and S.-C. Kong, "Modeling effects of operating conditions on biomass fast pyrolysis in bubbling fluidized bed reactors," *Energy & Fuels*, vol. 27, no. 10, pp. 5948–5956, 2013.
- [84] Q. Xiong and S.-C. Kong, "Modeling effects of interphase transport coefficients on biomass pyrolysis in fluidized beds," *Powder Technol.*, vol. 262, pp. 96–105, 2014.
- [85] Q. Xiong, S. Aramideh, and S. Kong, "Assessment of devolatilization schemes in predicting product yields of biomass fast pyrolysis," *Environ. Prog. Sustain. Energy*, vol. 33, no. 3, pp. 756–761, 2014.
- [86] Q. Xiong, F. Xu, E. Ramirez, S. Pannala, and C. S. Daw, "Modeling the impact of bubbling bed hydrodynamics on tar yield and its fluctuations during biomass fast pyrolysis," *Fuel*, vol. 164, pp. 11–17, 2016.
- [87] Q. Xiong, J. Zhang, F. Xu, G. Wiggins, and C. S. Daw, "Coupling DAEM and CFD for simulating biomass fast pyrolysis in fluidized beds," *J. Anal. Appl. Pyrolysis*, vol. 117, pp. 176–181, 2016.
- [88] Y. C. Yan, X. Y. Lim, W. Rashmi, and C. H. Lim, "Computational studies to investigate the fuel feeding point in fluidized bed reactor," *J. Eng. Sci. Technol.*, vol. 10, pp. 19–31, 2015.
- [89] Y. R. Lee, H. S. Choi, H. C. Park, and J. E. Lee, "A numerical study on biomass fast pyrolysis process: a comparison between full lumped modeling and hybrid modeling combined with CFD," *Comput. Chem. Eng.*, vol. 82, pp. 202–215, 2015.
- [90] P. Ranganathan and S. Gu, "Computational fluid dynamics modelling of biomass fast pyrolysis in fluidised bed reactors, focusing different kinetic schemes," *Bioresour. Technol.*, vol. 213, pp. 333–341, 2016.
- [91] C. Di Blasi, "Kinetic and heat transfer control in the slow and flash pyrolysis of solids," *Ind. Eng. Chem. Res.*, vol. 35, no. 1, pp. 37–46, 1996.
- [92] E. Ranzi *et al.*, "Chemical Kinetics of Biomass Pyrolysis," *Energy & Fuels*, vol. 22, pp. 4292–4300, 2008, doi: 10.1021/EF800551T.
- [93] A. Sharma, S. Wang, V. Pareek, H. Yang, and D. Zhang, "Multi-fluid reactive modeling of fluidized bed pyrolysis process," *Chem. Eng. Sci.*, vol. 123, pp. 311–321, 2015.
- [94] C. Di Blasi and C. Branca, "Kinetics of primary product formation from wood pyrolysis," *Ind. Eng. Chem. Res.*, vol. 40, no. 23, pp. 5547–5556, 2001.
- [95] S. Azizi and D. Mowla, "Cfd modeling of algae flash pyrolysis in the batch fluidized bed reactor including heat carrier particles," *Int. J. Chem. React. Eng.*, vol. 14, no. 1, pp. 463–480, 2016.
- [96] J. E. Lee, H. C. Park, and H. S. Choi, "Numerical study on fast pyrolysis of lignocellulosic biomass with varying column size of bubbling fluidized bed," *ACS Sustain. Chem. Eng.*, vol. 5, no. 3, pp. 2196–2204, 2017.
- [97] Q. Eri, B. Wang, J. Peng, X. Zhao, and T. Li, "Detailed CFD modelling of fast pyrolysis of different biomass types in fluidized bed reactors," *Can. J. Chem. Eng.*, vol. 96, no. 9, pp. 2043–2052, 2018.
- [98] A. Trendewicz, R. Evans, A. Dutta, R. Sykes, D. Carpenter, and R. Braun, "Evaluating the effect of potassium on cellulose pyrolysis reaction kinetics," *Biomass and bioenergy*, vol. 74, pp. 15–25, 2015.